Cost-Effective Processing of Flexible Tactile Sensors for e-skin Applications

Sachin[1,2], Sumit Choudhary[1,2], Ranbir Singh[1,2], Gopi Shrikanth Reddy[1,2], and Satinder K. Sharma[1,2]
[1]Indian Institute of Technology, Mandi, India
[2]IIT Mandi iHub and HCI Foundation, Mandi, India

2024 8th IEEE Electron Devices Technology & Manufacturing Conference (EDTM) | 979-8-3503-7152-9/24/$31.00 ©2024 IEEE | DOI: 10.1109/EDTM58488.2024.10512323

Abstract

Research into humanoid robotics explores interactive artificial smart skins that detect real-life cues and interact with humans. This study delves into a cost-effective approach for creating e-skin sensors, particularly utilizing room-temperature liquid metal in various sensory configurations. Proposing a novel Gallium-Indium-tin alloy (Galinstan) microfluidic sensor employs PDMS microchannels filled with Galinstan, offering stretchability, high sensitivity, and skin-mountable properties. The prototype processing involves using slender nylon threads within cross-linked PDMS to craft microchannel patterns. Liquid metal-based sensor demonstrates resilience, flexibility, and accurate detection of force and temperature variations, holding promising applications in robotics and healthcare. The promising facile, cost-effective process integration for these e-skin sensors realization is discussed in this article.

Keywords: Artificial skin, Galinstan, Tactile sensor, e-skin.

Introduction

Microchannel-based flexible sensors have gained noteworthy attention as a solution to the limitations of rigid sensors, which suffer from poor deformation and flexibility. The recent hike in applications in soft robotics, wearable consumer electronics, prosthetics, and electronic skins. The criterion for developing flexible and stretchable sensors become more stringent. The flexible sensors must exhibit low modulus, be lightweight, and have high flexibility and stretchability [1]–[4]. The various methods for designing complex microchannel systems are proposed and practised, including the lithographic approach, involving the creation of patterns on 2-D layers and their subsequent alignment, attachment, fusion, or locking of individual layers to form 3-D structures, which has gained popularity recently [5]. An alternative approach involves the application of a gold layer onto a substrate through the use of a patterned stamp. This method generates precise 3-D networks by layering planar structures on top of one another. The lithographic technique stands as the most commonly employed method for constructing microchannel systems with intricate topologies. In this procedure, patterns are initially crafted on 2-D layers and subsequently aligned, connected, fused, or secured to form 3-D structures. Another method entails imprinting a gold layer onto a substrate using a patterned stamp, resulting in planar structures constructed in layers to establish accurate 3-D networks [6]. While these methods prove efficient and yield diverse structures on both rigid and soft platforms, but they do have integration drawbacks, such as the inability to produce monolithic structures and challenges related to misalignment and interface sealing failures. An alternative approach to overcoming these challenges involves utilizing lasers for the internal modification of transparent materials like glass and quartz, followed by etching to create embedded 3-D structures. Laser scanning lithography has also been applied to shape flexible substrates, such as hydrogels, in both 2-D and 3-D [7]. This method prevents material contamination during processing, it requires specialized and costly equipment and may not be suitable for large-area rapid prototyping. Introducing a novel technique in this context, it draws inspiration from the observation that slender nylon fibers can be embedded inside a mold created through 3D printing. By pouring poly(dimethylsiloxane) (PDMS) into the mold and subsequently removing the fibers with minimal stress, microchannels are formed within the PDMS. Methods have been developed based on this principle to generate monolithic cylindrical microchannels with diameters ranging from 50 to 250 μm. This approach relies on two key principles: the limited adhesion of nylon to PDMS and the reversible, selective swelling of the PDMS network through solvents like chloroform and trimethylamine. This process integration keeps the nylon fiber unaffected, facilitating its easy removal from the cured PDMS substrate, thereby preserving the microchannel formed within the substrate [8].

Liquid metals, specifically gallium-based alloys (e.g., eutectic gallium indium alloy and gallium indium tin alloy), fulfill the specified criteria for flexible sensing applications, as outlined in Table 1 [9][10]. Gallium-based liquid metals exhibit biocompatibility and chemical stability, making them suitable for various applications, including intelligent wearable electronic devices, biosensors, biomedicine, and skin therapy. While the integration of flexible and wearable liquid metal-based sensors is a recent development in microfluidics, its advancement in the field of flexible electronics is rapidly progressing [11]. This study leverages microstructures for patterning and embedding liquid metals, employing a flexible and wearable sensor design to develop a functional skin-like tactile sensor. The step-by-step fabrication process, from substrate formation to intricate mold creation, metal filling, connection establishment, and thorough sensor characterization, underscores the precision and innovation involved in developing the skin-like tactile sensor for e-skin and wearable electronics applications.

Table 1: Properties of various liquid metals [12].

Material	Melting Point [°C]	Viscosity [Pa s]	Conductivity [S m^{-1}]	Thermal Conductivity [W m^{-1} K^{-1}]	Density [g cm^{-3}]
Mercury	-38.8	1.53×10^{-3}	1.04×10^{6}	8.5	13.55
Gallium	29.8	1.37×10^{-3}	6.73×10^{6}	29.3	6.09
Rubidium	38.9	N/A	7.79×10^{6}	58.2	1.532
Cesium	28.4	N/A	N/A	N/A	1.8785
EGaIn	15.5	1.99×10^{-3}	3.40×10^{6}	26.6	6.28
Galinstan	13.2	2.40×10^{-3}	3.46×10^{6}	16.5	6.44

Fabrication Process & Method

A. Formation of Substrate:

Soft and flexible platforms built of cross-linked poly-(dimethyl siloxane) (Sylgard 184, Dow Corning) were chosen for their beneficial features such as elasticity and

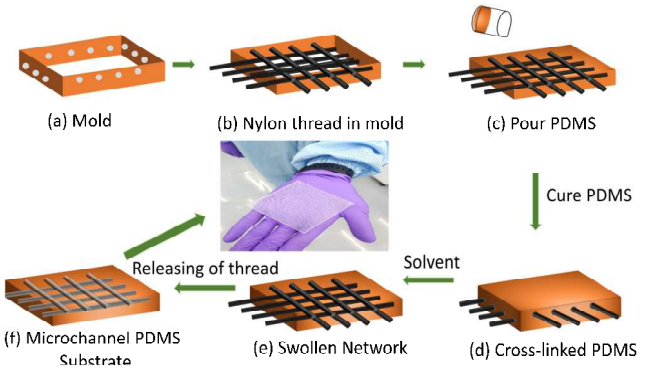

Fig. 1: Fabrication process of the wearable tactile sensor.

robustness. These platforms served as the core substrate for further microfluidic channel fabrication and processing.

B. Creation of Mold Using 3D Printing:

The meticulous design process of the 3D-printed mold aimed to match the overall thickness of the tactile sensor precisely, approximately 2 mm. This mold was systematically crafted using advanced 3D printing technology, ensuring accuracy in dimensions. Strategic placement of holes on opposite faces of the mold was employed to seamlessly accommodate slender nylon threads, each with a diameter ranging from 70 to 250 µm.

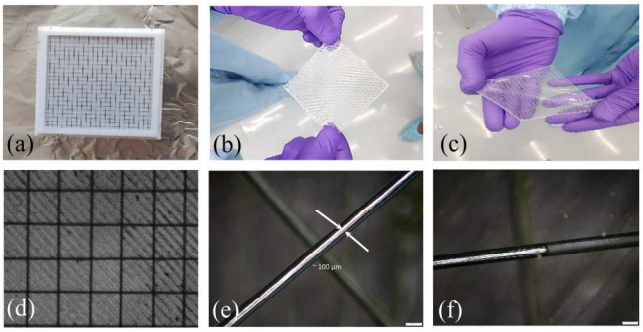

Fig. 2. (a) 3-D printed mold. (b, c) Flexible sensor with a grid of microchannel (d) Microscopic image of microchannels with dual plane microchannels for x-y motion. (e, f) Microchannel filled and partially filled with Galinstan, respectively.

C. Curing and Filling of Metal:

Following the scrupulous alignment of nylon threads within the mold, the polydimethylsiloxane (PDMS) mixture was precisely poured into the mold. The subsequent curing process entailed exposing the PDMS to a controlled temperature of 50 degrees Celsius for 3 hours. This critical curing phase was essential for establishing the desired structural integrity of the microfluidic channels. Concurrently, Galinstan liquid metal, comprising Ga:In:Sn = 62:22:16 wt %, was introduced into the microfluidic channels through a syringe pump, injecting approximately 0.1 ml of Galinstan in each channel.

D. Making Connections:

To ensure seamless integration with external devices, a modest approach was employed. A pair of silver-plated copper wires were strategically introduced into designated inlet/outlet holes, establishing reliable electrical connections

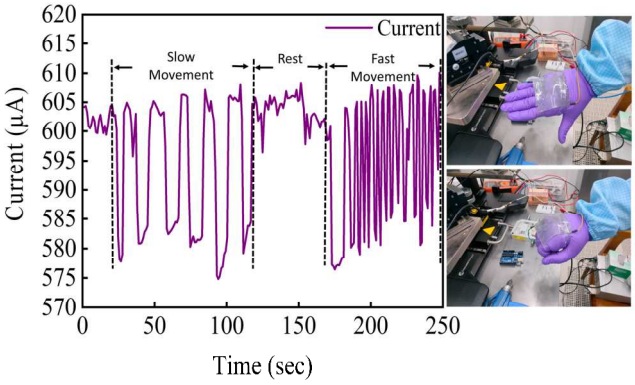

Fig. 3: Variation in current with slow and fast hand movements.

with the liquid-metal electrodes. This meticulous wiring process facilitated the sensor's seamless integration into external systems.

E. Characterizations:

The resultant tactile sensor, designed to mimic skin-like qualities, exhibited strain-sensing capabilities, boasting channel dimensions of 100µm×100µm with 20 channels in both the x and y directions filled with Galinstan. The sensor's patch overall dimensions were measured at 6.5×6.5cm, featuring a thickness of 2 mm. Its unique attributes, encompassing a melting point of 13.2°C and an electrical conductivity of 3.4×10^{-4} $S\cdot cm^{-1}$, underwent thorough characterization. This characterization process utilizes an Arduino microcontroller and Keithley 4200 SCS, ensuring precision in measurements and validating performance.

Result and Discussion

To comprehensively assess the performance of the prototype microfluidic tactile sensors, we systematically identified and characterized a set of key performance indicators. These crucial indicators encompass strain sensing, temperature sensing, and human hand motion sensing. The electrical characterization of the meticulously fabricated and integrated sensors was executed using the Keithley 4200 SCS cascaded with a probe station. This involved capturing current variations induced by hand bending during both rapid and gradual movements. The sensor, strategically positioned and tied on the human hand, utilized liquid metal embedded in the PDMS to deform linearly under the influence of hand movement, as shown in Fig. 3 Insets. Under normal conditions, when the sensor retains its original shape without deformation, the average current measures at 600 µA. As the hand undergoes gradual bending, the current experiences a decrement, reaching a minimum of 584 µA. This is possibly due to liquid metal resistance change. The recorded responses span both slow and fast movements, unveiling that the number of cycles for current changes escalates rapidly during rapid hand movement. This results in an average current of 605 µA in the normal hand position and a reduced 584 µA while bending. This observation underscores the sensor's remarkable capability to discern even the slightest deformation in its shape induced by human hand movement.

In evaluating the strain sensing capabilities, the sensor patch underwent a gradual stretch from 0 to 100% strain without any failure/deformation. This involved incremental straining, moving from the initial position at 6 cm to the maximum

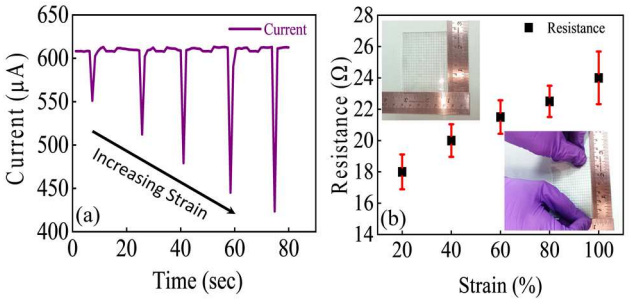

Fig. 4: (a) Change in current with increase in strain. (b) Resistance change w.r.t. variation in strain. Insets depicts the images for estimation of the strain for different lengths.

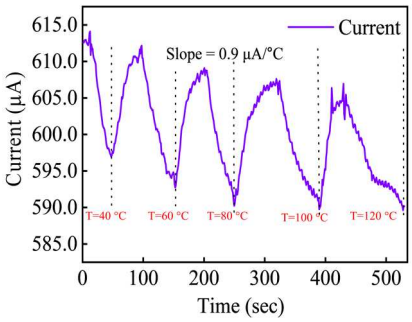

Fig. 5: Change in current with change in temperature.

strained state at 10 cm, with a systematic 20% increment at each step. The corresponding changes in current values were meticulously documented in Fig. 4(a). The results showcased the remarkable adaptability of Galinstan, effectively tracking the elastic deformation of the microchannel, as evidenced by the increase in resistance from 18 Ω to 24 Ω throughout the stretching process. The change in resistance was computed using Ohm's law (V=IR), as illustrated in Fig. 4(b). Impressively, the strain sensor demonstrated significant stability and durability during the stretching regimen, positioning undergoes resistance change. This demonstrates a promising candidate for artificial skin in robotic applications.

Additionally, to measure the actual change in current with temperature more accurately, we placed the tactile sensor on the LINKAM stage with a heating ramp rate of 50°C/min and recorded the change in current with the temperature variation. For this purpose, LINKAM heating stage model number LTS420E is employed, varying the temperature between 40 to 120 degrees in 20-degree increments, with responses recorded at each temperature interval. The results indicate that temperature sensitivity extracted through slope 0.9µA/°C, which means that for a 1°C rise in temperature, ~0.9 µA change in current was observed as depicted in Fig. 5. The sensor patch reaching a minimum current of 593 µA at T=120°C and maximum at T=25°C which is 612 µA. Furthermore, the sensor exhibits a rapid response to both increases and decreases in temperature; the rapid decrease in temperature is achieved by flowing nitrogen through the heating element to cool the stage.

Conclusion

An artificial skin with exceptional elasticity was created by incorporating a liquid metal within its structure. This innovative design does not involve the stacking and bonding of two hyper-elastic silicone rubber layers. The facile fabrication route for Galinstan embedded microchannel with distinct patterns that demonstrate various sensing functions, including multi-axial strain, contact, pressure, and temperature sensing for quick prototyping.

Acknowledgements

The authors would like to acknowledge the IIT Mandi iHub and HCI Foundation, Project No. IITM/iHub & HCIF-IIT MANDI/GSR/431 for financial funding and Centre for Design and Fabrication of Electronic Devices (C4DFED), Indian Institute of Technology (IIT) Mandi, India for fabrication and characterization facilities.

References

[1] J. C. Yeo, J. Yu, Z. M. Koh, Z. Wang, and C. T. Lim, "Wearable tactile sensor based on flexible microfluidics," *Lab Chip*, vol. 16, no. 17, pp. 3244–3250, 2016, doi: 10.1039/c6lc00579a.

[2] R. D. Ponce Wong, J. D. Posner, and V. J. Santos, "Flexible microfluidic normal force sensor skin for tactile feedback," *Sensors Actuators, A Phys.*, vol. 179, pp. 62–69, 2012, doi: 10.1016/j.sna.2012.03.023.

[3] L. Jamone, L. Natale, G. Metta, and G. Sandini, "Highly sensitive soft tactile sensors for an anthropomorphic robotic hand," *IEEE Sens. J.*, vol. 15, no. 8, pp. 4226–4233, 2015, doi: 10.1109/JSEN.2015.2417759.

[4] M. Xie *et al.*, "Flexible Multifunctional Sensors for Wearable and Robotic Applications," *Adv. Mater. Technol.*, vol. 4, no. 3, pp. 1–29, 2019, doi: 10.1002/admt.201800626.

[5] J. F. Ashley, N. B. Cramer, R. H. Davis, and C. N. Bowman, "Soft-lithography fabrication of microfluidic features using thiol-ene formulations," *Lab Chip*, vol. 11, no. 16, pp. 2772–2778, 2011, doi: 10.1039/c1lc20189a.

[6] S. Jeon *et al.*, "Three-dimensional nanofabrication with rubber stamps and conformable photomasks," *Adv. Mater.*, vol. 16, no. 15 SPEC. ISS., pp. 1369–1373, 2004, doi: 10.1002/adma.200400593.

[7] J. Ng, et al., "Components for integrated poly(dimethylsiloxane) microfluidic systems," *Electrophoresis*, vol. 23, no. 20, pp. 3461–3473, 2002, doi:10.1002/1522-2683(200210).

[8] M. K. S. Verma, A. Majumder, and A. Ghatak, "Embedded template-assisted fabrication of complex microchannels in PDMS and design of a microfluidic adhesive," *Langmuir*, vol. 22, no. 24, pp. 10291–10295, 2006, doi: 10.1021/la062516n.

[9] J. Dong, et. al. M. Wang, "Liquid metal-based devices: Material properties, fabrication and functionalities," *Nanomaterials*, vol. 11, no. 12, 2021, doi: 10.3390/nano11123400.

[10] Y. Wu *et al.*, "Liquid Metal-Based Strain Sensor with Ultralow Detection Limit for Human–Machine Interface Applications," *Adv. Intell. Syst.*, vol. 3, no. 10, pp. 1–8, 2021, doi: 10.1002/aisy.202000235.

[11] Y. G. Park, G. Y. Lee, J. Jang, S. M. Yun, E. Kim, and J. U. Park, "Liquid Metal-Based Soft Electronics for Wearable Healthcare," *Adv. Healthc. Mater.*, vol. 10, no. 17, pp. 1–26, 2021, doi: 10.1002/adhm.202002280.

[12] L. Zhu, B. Wang, S. Handschuh-Wang, and X. Zhou, "Liquid Metal–Based Soft Microfluidics," *Small*, vol. 16, no. 9, pp. 1–32, 2020, doi: 10.1002/smll.201903841.